



Advanced Stirling Converter Testing at NASA Glenn Research Center

*Salvatore M. Oriti and Gina M. Blaze
Glenn Research Center, Cleveland, Ohio*

NASA STI Program . . . in Profile

Since its founding, NASA has been dedicated to the advancement of aeronautics and space science. The NASA Scientific and Technical Information (STI) program plays a key part in helping NASA maintain this important role.

The NASA STI Program operates under the auspices of the Agency Chief Information Officer. It collects, organizes, provides for archiving, and disseminates NASA's STI. The NASA STI program provides access to the NASA Aeronautics and Space Database and its public interface, the NASA Technical Reports Server, thus providing one of the largest collections of aeronautical and space science STI in the world. Results are published in both non-NASA channels and by NASA in the NASA STI Report Series, which includes the following report types:

- **TECHNICAL PUBLICATION.** Reports of completed research or a major significant phase of research that present the results of NASA programs and include extensive data or theoretical analysis. Includes compilations of significant scientific and technical data and information deemed to be of continuing reference value. NASA counterpart of peer-reviewed formal professional papers but has less stringent limitations on manuscript length and extent of graphic presentations.
- **TECHNICAL MEMORANDUM.** Scientific and technical findings that are preliminary or of specialized interest, e.g., quick release reports, working papers, and bibliographies that contain minimal annotation. Does not contain extensive analysis.
- **CONTRACTOR REPORT.** Scientific and technical findings by NASA-sponsored contractors and grantees.

- **CONFERENCE PUBLICATION.** Collected papers from scientific and technical conferences, symposia, seminars, or other meetings sponsored or cosponsored by NASA.
- **SPECIAL PUBLICATION.** Scientific, technical, or historical information from NASA programs, projects, and missions, often concerned with subjects having substantial public interest.
- **TECHNICAL TRANSLATION.** English-language translations of foreign scientific and technical material pertinent to NASA's mission.

Specialized services also include creating custom thesauri, building customized databases, organizing and publishing research results.

For more information about the NASA STI program, see the following:

- Access the NASA STI program home page at <http://www.sti.nasa.gov>
- E-mail your question via the Internet to help@sti.nasa.gov
- Fax your question to the NASA STI Help Desk at 301-621-0134
- Telephone the NASA STI Help Desk at 301-621-0390
- Write to:
NASA Center for AeroSpace Information (CASI)
7115 Standard Drive
Hanover, MD 21076-1320



Advanced Stirling Converter Testing at NASA Glenn Research Center

*Salvatore M. Oriti and Gina M. Blaze
Glenn Research Center, Cleveland, Ohio*

Prepared for the
Fifth International Energy Conversion Engineering Conference and Exhibit (IECEC)
sponsored by the American Institute of Aeronautics and Astronautics
St. Louis, Missouri, June 25–27, 2007

National Aeronautics and
Space Administration

Glenn Research Center
Cleveland, Ohio 44135

Acknowledgments

The work described in this paper was performed for the Science Mission Directorate (SMD) and the Radioisotope Power System (RPS) Program, which provided funding for these projects.

Trade names and trademarks are used in this report for identification only. Their usage does not constitute an official endorsement, either expressed or implied, by the National Aeronautics and Space Administration.

Level of Review: This material has been technically reviewed by technical management.

Available from

NASA Center for Aerospace Information
7115 Standard Drive
Hanover, MD 21076-1320

National Technical Information Service
5285 Port Royal Road
Springfield, VA 22161

Available electronically at <http://gltrs.grc.nasa.gov>

Advanced Stirling Converter Testing at NASA Glenn Research Center

Salvatore M. Oriti and Gina M. Blaze
National Aeronautics and Space Administration
Glenn Research Center
Cleveland, Ohio, 44135

Abstract

The U.S. Department of Energy (DOE), Lockheed Martin Space Systems (LMSS), Sunpower Inc., and NASA Glenn Research Center (GRC) have been developing an Advanced Stirling Radioisotope Generator (ASRG) for use as a power system on space science and exploration missions. This generator will make use of the free-piston Stirling converters to achieve higher conversion efficiency than currently available alternatives. The ASRG will utilize two Advanced Stirling Convertors (ASC) to convert thermal energy from a radioisotope heat source to electricity. NASA GRC has initiated several experiments to demonstrate the functionality of the ASC, including: in-air extended operation, thermal vacuum extended operation, and ASRG simulation for mobile applications. The in-air and thermal vacuum test articles are intended to provide convertor performance data over an extended operating time. These test articles mimic some features of the ASRG without the requirement of low system mass. Operation in thermal vacuum adds the element of simulating deep space. This test article is being used to gather convertor performance and thermal data in a relevant environment. The ASRG simulator was designed to incorporate a minimum amount of support equipment, allowing integration onto devices powered directly by the convertors, such as a rover. This paper discusses the design, fabrication, and implementation of these experiments.

Nomenclature

LMSS	Lockheed Martin Space Systems
FET	Field-Effect Transistor
DOE	Department of Energy
PWM	Pulse Width Modulator
ASC	Advanced Stirling Converter
μF	micro farad
ASRG	Advanced Stirling Radioisotope Generator
RMS	root mean square
RTG	Radioisotope Thermoelectric Generator
W_e	watt electric
GPHS	General Purpose Heat Source
NASA	National Aeronautics and Space Administration
GRC	Glenn Research Center
FTB	Frequency Test Bed
TDC	Technology Demonstration Converter
DAQ	Data Acquisition
FPC	Failsafe Protection Circuit
PID	Proportional-Integral-Derivative
W_{th}	watt thermal
psi	pound per square inch
FEA	finite element analysis
W/cm^2	watt per square centimeter
CTE	coefficient of thermal expansion
V_{AC}	volt, alternating current
Hz	hertz
V_{DC}	volt, direct current

I. Introduction

Lockheed Martin Space Systems (LMSS) was selected as the system integration contractor by the Department of Energy (DOE) to develop a radioisotope-powered generator for potential use on space science and exploration missions¹. This generator will utilize Advanced Stirling Convertors (ASC) to convert heat from a radioisotope source into electricity, and thus has been named the Advanced Stirling Radioisotope Generator (ASRG). The ASCs were designed and fabricated by Sunpower, Inc. of Athens, Ohio. Stirling power conversion offers a four fold increase in efficiency over Radioisotope Thermoelectric Generators (RTGs), requiring one fourth the amount of radioisotope fuel for the same power output¹. LMSS's design of the ASRG engineering unit is shown in Fig. 1. The engineering unit will use electric heaters to simulate the Plutonium-238 General Purpose Heat Source (GPHS) modules that will be used in flight. One heat source is coupled to each ASC. Some candidate missions require continuous operation of the power system for up to 14 years, with an additional 3 years of storage prior to launch. Because of this long life requirement, several experiments have been initiated at NASA Glenn Research Center (GRC) to demonstrate life and reliability of the ASC^{2,3}. One testing technique implemented involves continuous, unattended convertor operation to gather performance data over a period of thousands of hours. Continuous operation allows observation of convertor operating trends over a sufficient length of time to confirm or dismiss the presence of degradation.

The following sections will describe three unique test article designs. Two of these were designed for continuous operation, one for an in-air environment and another for a thermal vacuum environment. The third test article was designed to simulate the ASRG for the purposes of short-term demonstrations outside the laboratory. The experiments were designed to allow adjustment of operating conditions, including: hot-end and rejection temperatures, piston amplitude of oscillation, and mean charge pressure of the working gas. Each test article was instrumented to measure these parameters and all output characteristics, such as alternator voltage, alternator current, operating frequency, and power. Each uses electric heaters to supply thermal energy to the convertors, making power input measurements simple and accurate. The test articles differ primarily in their methods of cycle heat rejection. The in-air test article rejects heat to a coolant loop through which a temperature controlled fluid is circulated. The thermal vacuum test article utilizes radiator panels that dissipate the waste heat to a liquid nitrogen cooled shroud. The ASRG simulator rejects heat by flowing room-temperature air through fins attached to the rejection ends of the convertors.

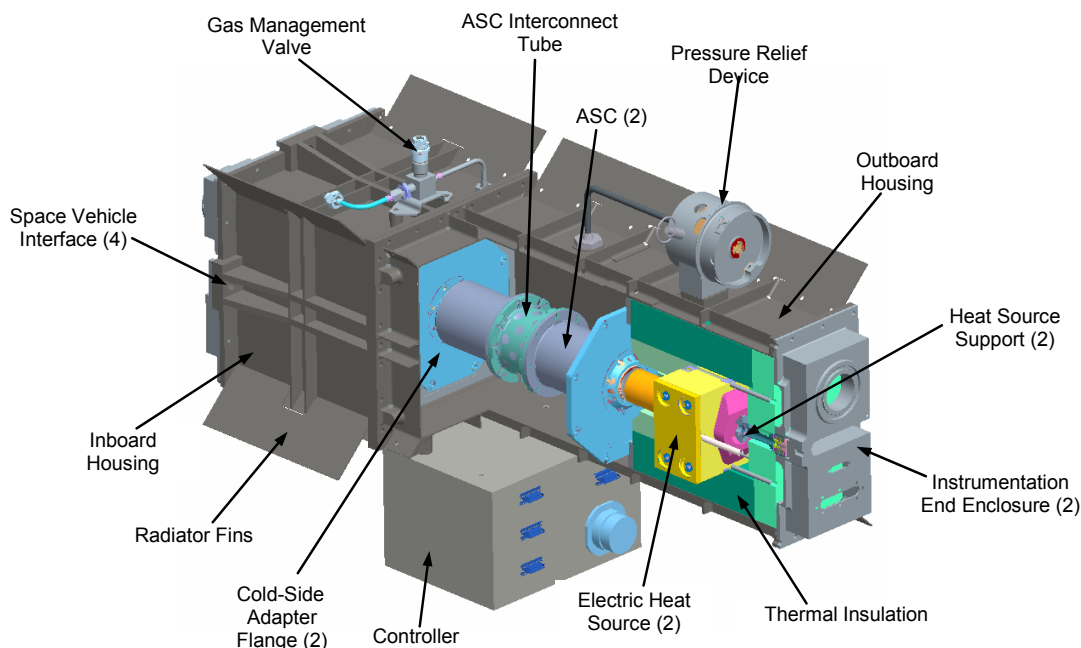


Figure 1.—LMSS Advanced Stirling Radioisotope Generator Engineering Unit. One electric heat source is coupled to each ASC.

Three versions of ASC prototypes are available for these experiments, as summarized in Table 1. ASC-0 units have Inconel 718 (Special Metals) heater heads with a maximum hot-end temperature of 650 °C while ASC-1HS units have MarM-247 heater heads with a maximum hot-end temperature of 850 °C. The ASC-0 and ASC-1HS units were hermetically sealed by welding the flange joints. Frequency Test Bed (FTB) units are non-hermetically sealed development units⁴ with stainless steel heater heads and a maximum hot-end temperature of 550 °C. These units are used in the ASRG simulator.

TABLE 1.—ADVANCED STIRLING CONVERTOR ASSETS AT GRC.

Convertor model	Heater head material	Hermetic	Hot-end temperature, °C	Operation
ASC-0	Inconel 718	Y	650	Extended
ASC-1HS	MarM-247	Y	850	Extended
FTB	Stainless Steel	N	550	ASRG simulator

II. Extended Operation Test Stations

Capability for continuous, unattended operation of Stirling convertors was first developed at GRC in 2003 to support Technology Demonstration Convertor (TDC) testing during the 110 W_e SRG project⁵. The project was redirected in May 2006 to increase specific power of the generator by using ASC technology¹. The knowledge and experience acquired during TDC testing was applied to ASC testing. Each test station in the GRC Stirling Research Lab includes an operations rack, support stand, gas management components, and test article of interest. A test station with an ASC-0 test article is shown in Fig. 2. The Stirling Research Lab at GRC contains four of these test stations. A total of eight ASCs may be operated simultaneously; three pairs in-air and a fourth pair in thermal vacuum.

All test articles described in this paper orient a pair of convertors in the dual-opposed configuration, with the heater heads facing outward and the pressure vessel sections rigidly attached to each other. This configuration permits operation at near zero net vibration because the piston motions are equal but opposite in direction to achieve dynamic balance. This is also the orientation of the convertor pair in the ASRG.

The operations rack comprises the data system, hard-wired failsafe protection devices, hot-end temperature control systems, transducers, and convertor controller with parasitic load. The data system was based on National Instruments software and hardware. The LabVIEW-based (National Instruments) data acquisition (DAQ) software was developed to operate in unattended mode and is capable of controlling the support systems without user intervention. The user may specify upper and lower bounds for any parameter monitored by the DAQ system. The DAQ software will safely shut down operation of the test article when an out-of-bounds condition is sensed. Parameters that may trigger a shut down include: hot-end and rejection temperatures, convertor mean charge pressure, piston amplitude of oscillation, and loss of building power.

Hard-wired protection devices were also installed in the operations rack that function independent of the software-based protection. The hot-end temperature of each convertor is monitored by a limit controller. If either hot-end temperature exceeds the user-defined limit, the limit controller removes heater power from both convertors via a relay. A failsafe protection circuit (FPC) was implemented to prevent piston over-stroke. The FPC is capable of monitoring up to five input signals. Each input has an associated, user-adjustable set-point. When any signal exceeds its set-point, an emergency load is applied across both alternators in less than one-half of a cycle. Piston position sensor signals are the primary input. However, other signals may also be used, such as accelerometer or alternator voltage.

Hot-end temperature control is accomplished by use of programmable DC power supplies driven by closed-loop proportional-integral-derivative (PID) controllers. Each hot-end temperature is controlled individually. Power input and output are measured using voltage, current and power transducers. The transducers output signals ranging from zero to five volts that are recorded by the DAQ system.



Figure 2.—Extended operation test station. A pair of ASC-0 units setup for continuous unattended operation in air.

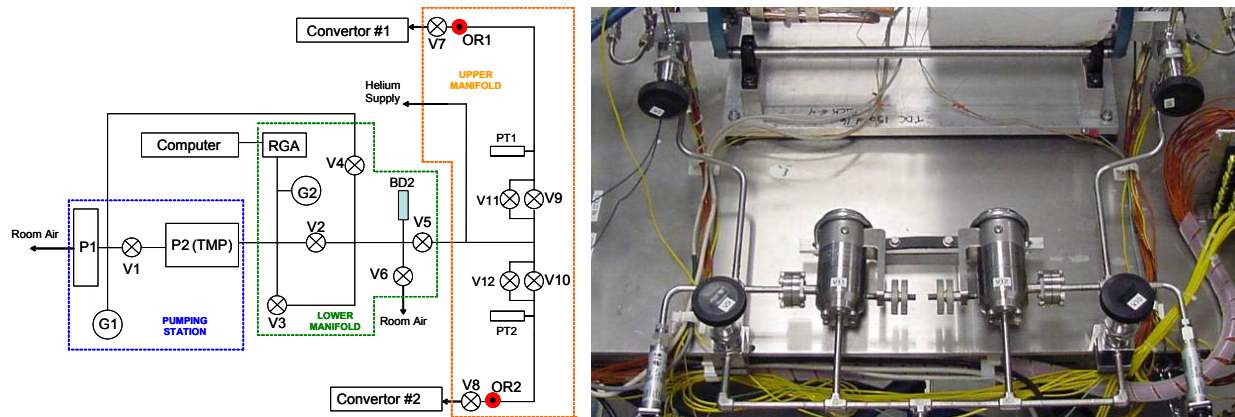


Figure 3.—Helium management system. System schematic (left) and photograph of upper manifold on support stand (right).

Convertor control is performed by a zener-diode power electronics controller that allows user adjustment of the piston amplitude via a variable zener-diode. The controller’s parasitic load was situated in the operations rack and dissipates all the unused power produced by the test article.

The working gas of the hermetically sealed units (ASC-0 and ASC-1HS) is still accessible via a fill tube and isolation valve attached to each convertor. The isolation valve allows a convertor to be disconnected from the test stand without sacrificing its high purity charge. During extended operation, the convertors are connected to a helium management system with the isolation valves open (V7 and V8 of Fig. 3). A 0.0004 in. diameter orifice was installed on the inlet fitting of each isolation valve to prevent bounce space pressure wave communication to the manifold. The helium management system serves the functions of convertor evacuation during bakeout, evacuation of system tubing, charge pressure adjustment, and sampling of the working gas.

A. In-Air ASC Operation

The in-air ASC test article is shown Fig. 4. Two ASC’s were mounted in the dual-opposed configuration using the tabs on the pressure vessels. The spacing between the convertors was sized for thermal vacuum operation, which will be described in the next section. On the thermal vacuum test article, the space between the convertors is occupied by the controller and a portion of the radiator panel assemblies.

The heat rejection system consists of a copper rejection flange attached to the convertor, aluminum coolant collars, and temperature controlled circulator. The rejection flange was brazed to the rejection zone of the ASC heater head during fabrication. The coolant collars were clamped into the circumferential groove of the rejection flange by 12 fasteners. Coolant lines were connected to the inlets and outlets of the collars. One circulator located below the support stand provides coolant to both convertors Fig. 2. The other circulator is a spare that may be used for pressure vessel temperature control at a later time. The heat from the rejection portion of the cycle is conducted away from the heater head by the copper flange and into the aluminum collars. The coolant circulated through the collars then absorbs the waste heat. The rejection temperature of the convertor is controlled by the coolant temperature. Ethylene glycol is used since the required fluid temperature ranges from 10 to 90 °C.

The heat rejection flange was designed in collaboration with Sunpower, Inc. The flange geometry was designed to adapt to the existing ASC design and satisfy the thermal requirements. The rejection hardware was designed to permit operation of the convertor in either air or thermal vacuum conditions. To achieve this, the flange was designed to accept either the collars that interface to a pumped coolant loop or radiator panels. For efficient heat rejection, the temperature drop across components should be minimized. The rejection flange was required to conduct $145 W_{th}$ with a temperature drop of 10 °C or less. This heat flow value represents a 10% margin over the nominal heat rejection of the ASC thermodynamic cycle. Copper was chosen for the flange material because of its high thermal conductivity and machinability. The flange’s circumferential groove geometry was driven by the requirement to supply 1400 psi of contact pressure to the cooling device. This value was based on heat transfer guidelines regarding copper and aluminum surfaces. The groove width was driven by the thickness of the radiator panels which will be discussed in the following section. Thermal finite element analysis (FEA), was used to predict a temperature drop of only 6.2 °C. The coolant collars were designed to occupy minimum space while permitting sufficient coolant flowrate to remove the cycle waste heat. The required coolant passage diameter was initially estimated at 0.25 in. This geometry was analyzed by modeling the passage as a straight duct with a constant wall

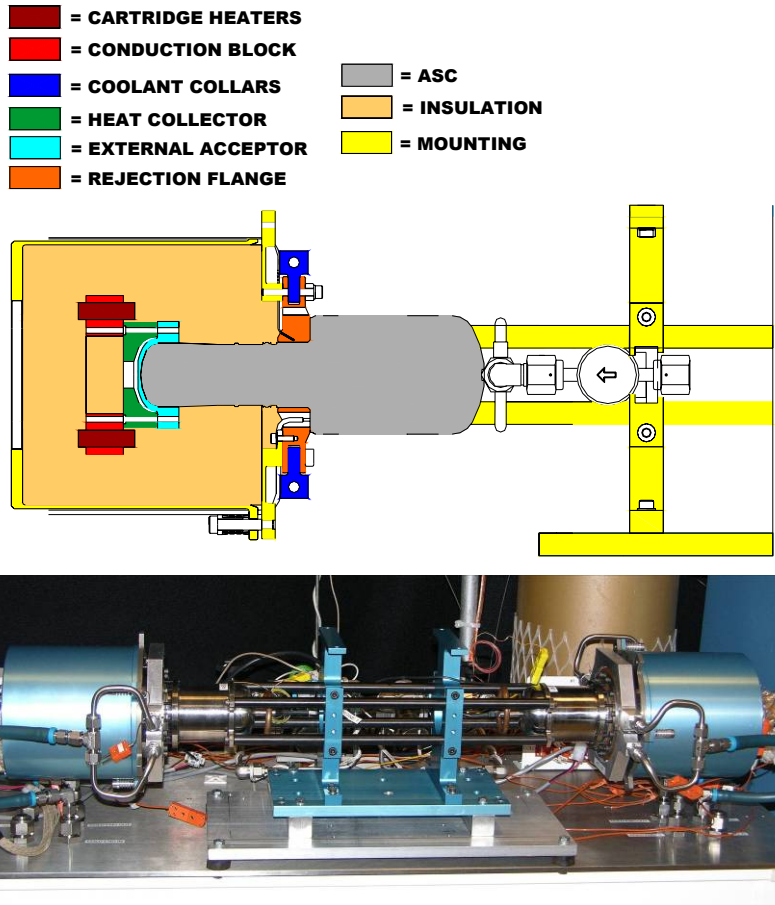


Figure 4.—ASC in-air test article. Assembly partial section view (top) and photograph (bottom).

temperature and underdeveloped laminar coolant flow. The analysis indicated marginally acceptable performance using ethylene glycol at a flowrate of 1 liter per minute. However, the rejection hardware performed adequately during testing, requiring only a 15 °C difference between the fluid and rejection temperatures at maximum power. One possible explanation is that the actual flow through the collars becomes turbulent, thereby increasing the heat transfer coefficient. Checkout testing of ASC-0 units in air revealed the heat rejection system was capable of maintaining the rejection temperature at any point between 50 and 90 °C while operating at maximum power. Operation at rejection temperatures below 50 °C was not explored.

The heat input hardware consists of a heat collector, external acceptor, and cartridge heater source. The heat collector and external acceptor form a two-piece brazed assembly that directs thermal energy to the input zone of the heater head. The cartridge heater source was preloaded onto the collector and acceptor assembly by threaded rods. The heat collector was designed to interface to two heat sources; cartridge array and Boralectric (GE Advanced Ceramics). The in-air heat source consists of an array of six cartridge heaters inserted into a copper or nickel block. The Boralectric heat source is specific to thermal vacuum operation, and will be described in the following section. Both heat sources required a flat surface on the exposed end of the heat collector. The flat heater interface was also desirable because it emulates use of the GPHS modules in the ASRG. Thermal FEA was used to determine overall thickness of the collector. The final geometry, shown in Fig. 4, was driven by structural analysis. The axial length of collector was made large enough so that it would not yield under load from the heater attachment while operating at maximum temperature. The hot-end and regenerator sections were insulated by Kaowool (Thermal Ceramics). An aluminum can was installed over the insulation bundle to maintain its shape and position.

Two ASC-0 units (S/N nos. 1 and 2) were received on December 20, 2006. After installation onto the test station, evacuation and fill was completed using the helium management system described in the previous section. The converters and manifold plumbing were evacuated down to 2.8×10^{-7} torr, then backfilled with ultra-high purity helium (99.999%) to 440 psig. It was estimated that this room-temperature charge pressure would result in 515 psig at full temperature and power. Operation of ASC-0 nos.1 and 2 at GRC was initiated on February 2, 2007. The

testing activities that followed included checkout of the controller and unattended operation software. Typically, the path to continuous, unattended mode operation includes two stages. The first is a low-temperature checkout during which the hot-end temperature is restricted to lower value than the full design temperature. Low-temperature checkout of ASC-0 nos.1 and 2 was performed at 550 °C hot-end and 50 °C rejection. These temperatures were chosen because 50 °C was the lowest recommended rejection temperature and 550 °C was the required hot-end temperature to achieve West number similitude with the full design condition. The second stage is a demonstration at the full temperature condition of 650 °C hot-end and 90 °C rejection. This was achieved on February 8, 2007, and continuous, unattended mode operation was initiated the same day. Operation continued until March 5, 2007 at which time operation was manually shut down after accumulating 600 hr.

Insulation loss characterization was then performed to calculate net efficiency by quantifying the portion of total thermal energy input that is delivered to the heater head. The remainder may be attributed to insulation losses that the engine cycle has no opportunity to convert to work. The insulation losses were calculated by evacuating the convertors, then measuring the thermal power required to maintain various temperature ratios (Table 2). Since there was no working gas, no thermal power could be drawn by the thermodynamic cycle. The evacuation also eliminated gas conduction and convection between internal heater head components. The amount of energy conducted and radiated down the heater head was calculated for each step of the matrix. Following insulation loss characterization, the convertors began the transition to thermal vacuum operation.

TABLE 2.—ASC-0 INSULATION LOSS CHARACTERIZATION TEMPERATURE MATRIX.

Point	Hot-end temperature, °C	Rejection temperature, °C
1	550	50
2	650	
3	550	90
4	650	

B. Thermal Vacuum ASC Operation

The thermal vacuum test article is shown in Fig. 5. Two convertors were mounted in the dual opposed configuration using on the same support structure used for in-air test article. The convertor pair was attached to a support stand that locates it in the center of the vacuum chamber and liquid nitrogen shroud. The test article was structurally isolated by wire rope isolators between the support stand and mounting. The liquid nitrogen shroud surrounds 100 percent of the test article. A zener-diode controller was integrated into the test article and fastened to the center supports. However, the controller's parasitic load remains outside the vacuum tank in the operations rack.

The heat rejection system utilizes aluminum radiator panels clamped into the circumferential groove of the rejection flange. The panels were coated with ECP-2200 to increase their emissivity to approximately 0.9. T-gon (Thermagon) 805 graphite sheets were installed at all copper-aluminum interfaces to reduce thermal contact resistances. The radiator panel geometry was analyzed with FEA, with the model including the dual-opposed convertors, the heat load from the cycle, insulation containers, pressure vessels, and controller. The liquid nitrogen shroud was simulated by applying a radiation sink temperature enclosing 100% of the model geometry. The panel geometry was adjusted to maintain the rejection temperature at 90 °C while dissipating 145 W_{th} in this environment.

The heat input system utilizes a Boralectric heater instead of the cartridge heater source (Fig. 6). Boralectric heaters are manufactured by encapsulating a pyrolytic graphite element in pyrolytic boron nitride. The heater geometry was designed with guidelines provided by the manufacturer. The lowest thermal resistance occurs at the outer perimeter of the heat collector, which drove the heater shape to the maximum allowable inner and outer diameters. The outer diameter was limited by the bolt pattern that attaches the heat source and the inner diameter was limited by manufacturability. The chosen geometry delivers full power at a heat flux of approximately 30 W/cm², which is 60% of the manufacturer's recommended maximum. The heater was preloaded onto the collector by a backing plate and six threaded rods. The fastener pattern is the same as that used to preload the cartridge heater source during in-air operation. The electrical connection was made by a threaded rod on each contact of the heater. These two rods function as the electrical paths that supply power to the heater. The backing plate and threaded rods were made of MarM-246, a nickel-based super alloy with properties very similar to MarM-247. Previous thermal vacuum testing at GRC revealed issues related to the relatively large coefficient of thermal expansion (CTE) of the Boralectric heater⁶. To mitigate this effect, molybdenum spacers were integrated into each fastened joint. Molybdenum was chosen because of its low CTE and high temperature capability. The spacers were

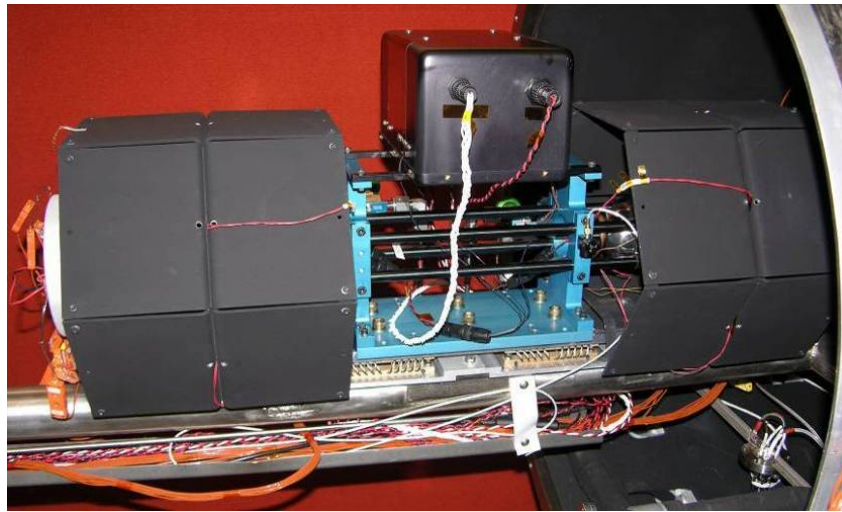
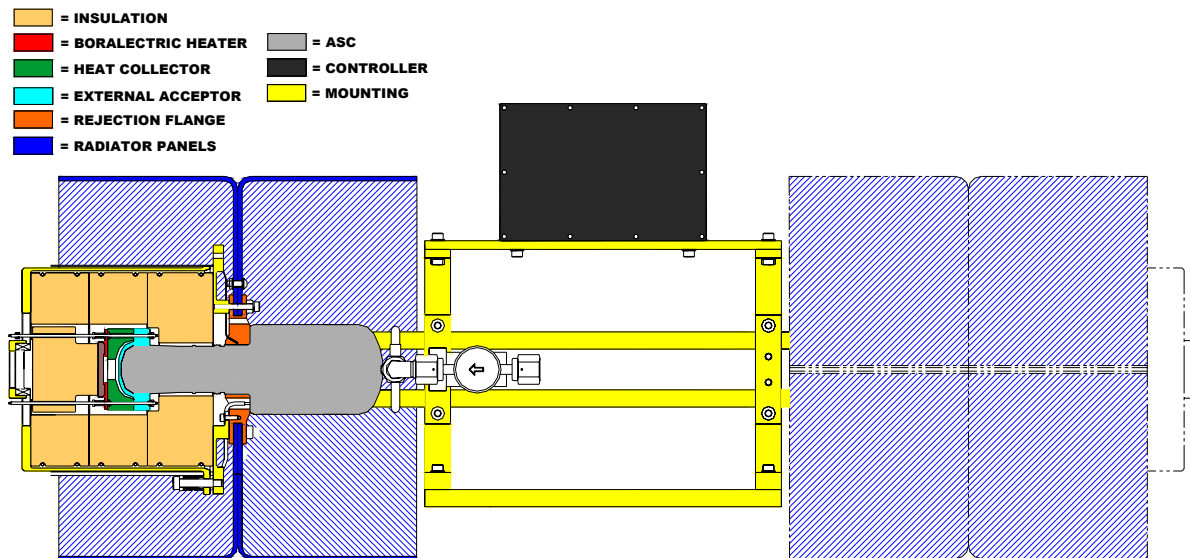


Figure 5.—ASC thermal vacuum test article. Assembly partial section view (top) and photograph (bottom).

sized so that the expansion of the threaded rods during temperature increases equaled the total expansion of the stack-up, eliminating thermally induced stresses.

The hot-end and regenerator sections were insulated by rigid, microporous insulation. The outer pieces assembled onto the ASC along the radial direction, and are compressed by six garter springs around the circumference. The volume above the heater was filled by insulation compressed by an externally loaded spring. Because the microporous insulation is rigid, it cannot conform to the minor contours of the ASC. Volumes that would be left void were filled with Kaowool ceramic blanket insulation. The insulation stack was compressed along the axial direction by a spring-loaded aluminum can.

Following the 600 hr of in-air operation, ASC-0 nos.1 and 2 were reconfigured with the thermal vacuum hardware. Operation of these units in thermal vacuum was achieved on March 30, 2007. Continuous operation was initiated on April 3, 2007. As of June 1, 2007, the converters have operated for over 1000 hr in thermal vacuum. All thermal vacuum hardware has performed as expected up to the full design hot-end temperature of 650 °C.

The ASC-1HS units will follow the same sequence of testing as ASC-0 nos. 1 and 2, but will not be operated in-air for an extended period of time. Instead, efforts will be concentrated operating them in thermal vacuum. The ASC-1HS units are anticipated to arrive during the summer of 2007. The use of MarM-247 as the heater head material will permit extended operation at a hot-end temperature of 850 °C.

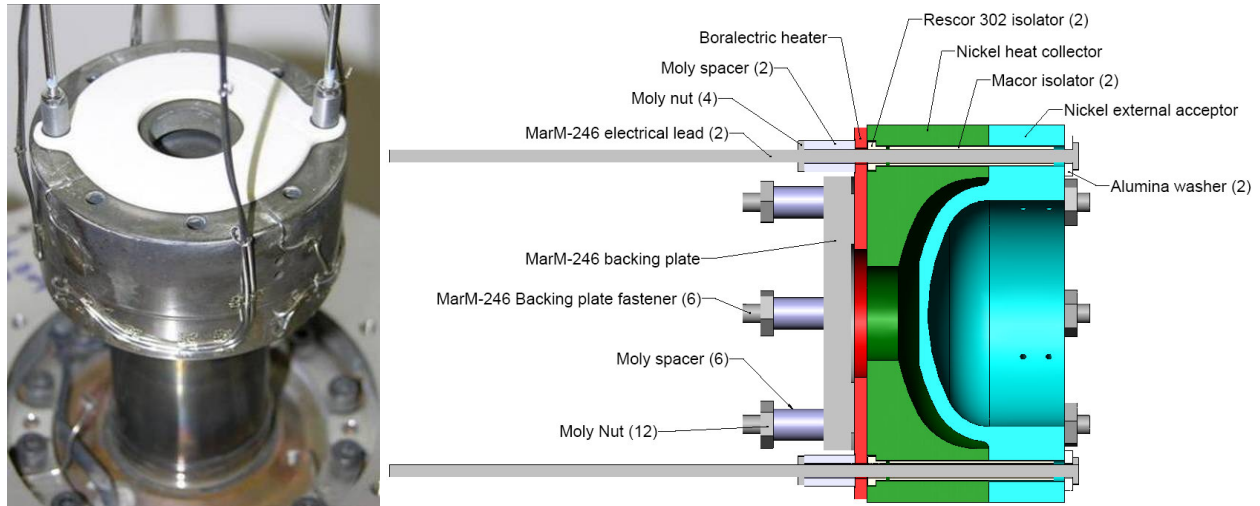


Figure 6.—Thermal vacuum heat source. Boralectric heater photograph (left) and assembly section view (right).

III.ASRG Simulator

An ASRG simulator was designed for demonstrating Stirling power conversion outside the laboratory environment. The setup is depicted in Fig. 7. Two FTB units were mounted in the dual-opposed configuration. Prior to delivery, these units were custom fit with fins on the rejection zone to permit air-cooling. The mounting structure serves the function of supporting the converters and providing containment for the air flow from the cooling fans. The outer panels of the containment were made of clear plastic to allow observation of the converters inside. Two fans located on the top of the container draw air in from the environment and discharge into the containment through the top panel. The cooling fins and fans were sized for operation in ambient air temperatures up to 110 °F.

Thermal energy is supplied to each hot end by an array of cartridge heaters inserted into a nickel heat collector. The hot end and regenerators sections were insulated using Kaowool ceramic blanket. An aluminum container was installed around the insulation package to maintain its shape. The inner insulation containment also functions to direct the air flow exiting the cooling fins along the radial direction.

A helium management system was integrated into the container for charge pressure adjustment. Included is a pressure gauge displaying the charge pressure of both converters, and an isolation valve. A fill port located on the opposite side of the container allows connection to a helium supply.

The ASRG simulator system was designed to require as little support equipment as possible, with the intended application being integration onto a rover. Operation of the ASRG simulator requires three supporting components: tuning capacitor bank, control electronics, and ground support equipment (Fig. 8). The tuning capacitor bank is necessary for power factor correction, and is connected in series with the alternator outputs. The control electronics contains the linear AC controller, protection circuit, and one of the two emergency stop switches. Power is supplied to the user by one of the connectors on the front of the control electronics. This output is regulated to 28 V_{DC} by a DC-DC converter. The controller's parasitic load is located on the sides of the container, and was designed to dissipate full power while being air-cooled by natural convection. Any power not absorbed by the user is dissipated in the parasitic load. The linear AC controller development will be discussed more the following section. The ground support equipment requires a connection to a 120 V_{AC}, 60 Hz source. It provides heater power and temperature control, cooling fan power, centering and starting circuits, and the second emergency stop switch. Each heater array is connected to 120 V_{AC} in series with a solid state relay. PID controllers vary the duty cycle of the solid state relays to maintain the hot-end temperature set-points. Over temperature protection is accomplished by using the alarm relay integrated into each PID controller. When either upper temperature limit is exceeded, the relay opens both heater circuits, removing power from the heaters.

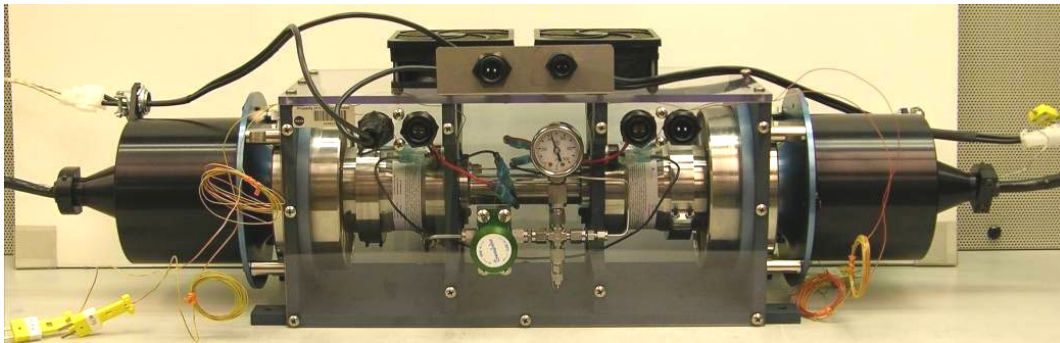
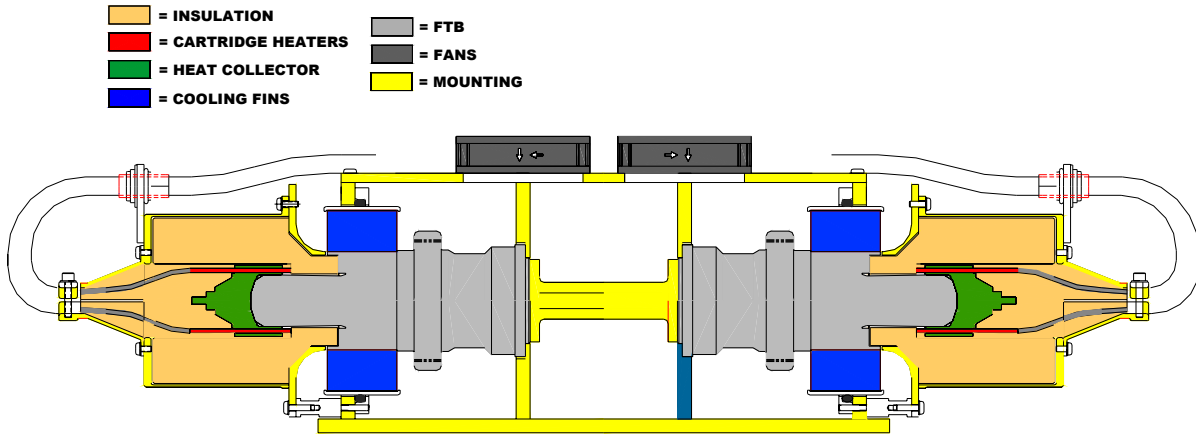


Figure 7.—ASRG Simulator. Assembly section view (top) and photograph (bottom).



Figure 8.—ASRG simulator support equipment. Tuning capacitor bank (top left), control electronics (top right), and ground support equipment (bottom).

The capacitor bank and control electronics are intended to be located on the device being powered along with the ASRG simulator. The ground support equipment may be located remotely and connected to the other components via an umbilical cable. Losses in the umbilical cable only affect the heater power, fan power, and hot-end temperature control thermocouples. Converter power output is unaffected since it never travels over the umbilical cable, but rather directly to the nearby controller and user loads. Since the heater and fan power is provided at

relatively low current, the line losses are negligible, even over a 30 m length of 16 gauge wire. The thermocouple signals traveling over this cable were also proven to be accurate and reliable through experimentation.

The ASRG simulator and support equipment buildup was completed in December 2006. In the same month, the convertors were operated up to a combined power level of 130 W_e. Use of the ASRG simulator for a rover demonstration is anticipated to take place during the summer of 2007.

IV. ASRG Simulator Controller Development

Free-piston Stirling convertors require controllers to maintain stable operation. During each cycle, the load must be modulated to precisely dissipate all the power being produced. If the controller did not dissipate all the power, the excess would flow into the resonating piston motion, increasing amplitude, and ultimately resulting in damage to internal convertor components. Similarly, if the controller dissipated more power than that being produced, the balance would be extracted from the resonating piston motion, ultimately causing a stall of the engine cycle. The controller also provides a regulated user voltage at its output. The majority of powered devices require direct current. Typically, to provide DC, the controller rectifies the alternator output, and then modulates the applied load to maintain a specified output voltage. Most controllers have a feature that allows the operator to change the piston amplitude of oscillation.

An in-house controller development effort was initiated in March 2006. The goal of this task was to design and build a small, efficient, and reliable controller for use on the ASRG simulator. This effort was entirely separate from the power factor correcting controller work performed previously at GRC. Each of the methods considered was analog and utilized tuning capacitors for passive power factor correction. No active power factor correcting control methods were investigated. The tuning capacitors passively correct the power factor by nullifying the effect of the alternator inductance. One important consequence of this technique is that the tuning capacitor will only cancel the effect of the alternator inductance at a single frequency. If the operating frequency deviates from this value, the power factor correction will be reduced.

Originally, each control concept was designed for TDC operation. The designs required modification to accommodate the lower alternator voltage and higher power output of the ASCs and FTB convertors. Each controller was designed for both single convertor and dual-opposed pair operation. The circuit simulation software PSpice (Cadence Design Systems) was used to simulate operation of an ASC convertor pair on each of the controllers. A model of each controller circuit connected to the ASC linear alternators was constructed. The linear alternator was modeled as an AC voltage source using its nominal values for resistance, inductance, frequency, and output voltage. The following control methods were considered:

1. Zener-Diode (Fig. 9)

The AC from both alternators is converted to DC by a diode bridge and an energy storage capacitor. The loads are then applied in stages to the DC bus. The DC voltage is connected to the operational amplifiers only after it exceeds the breakdown voltage of the zener-diode. The output of each operational amplifier controls the state of a field effect transistor (FET), which functions to switch a resistance onto the DC bus. The voltage level at which each operational amplifier turns on is controlled by sensing resistors, which are sized so that the trip point of each operational amplifier is slightly higher than the previous one. As the DC voltage rises above the first trip point, the first operational amplifier will turn on, applying its associated resistance to the DC bus. If the DC voltage continues to increase, the next operational amplifier in sequence will turn on, applying more load. This process continues until the DC voltage stops increasing or until all stages are on. As the DC voltage drops, the stages turn off one at a time in the reverse sequence. Because the DC voltage is produced by a rectified sine wave, the cycle of applying loads occurs at twice the convertor operating frequency. The load resistors are sized so that there is sufficient load available to maintain piston amplitude control at maximum convertor power output. The user may change the piston amplitude by adjusting the breakdown voltage of the zener-diode. Increasing the breakdown voltage of the zener-diode increases the ‘floor’ which the DC voltage must reach before any of the loads are activated. Therefore, the piston amplitudes can be increased by increasing the DC voltage. This control method was considered the baseline for the evaluation effort. The zener-diode controller has been used to operate several convertor designs and has heritage in the GRC Stirling Research Lab.

2. Linear DC Regulator (Fig. 10)

The linear DC regulator method functions much the same way as the zener-diode method, but applies load in a directly proportional manner, rather than in discrete steps. As with the zener-diode controller, the AC from both

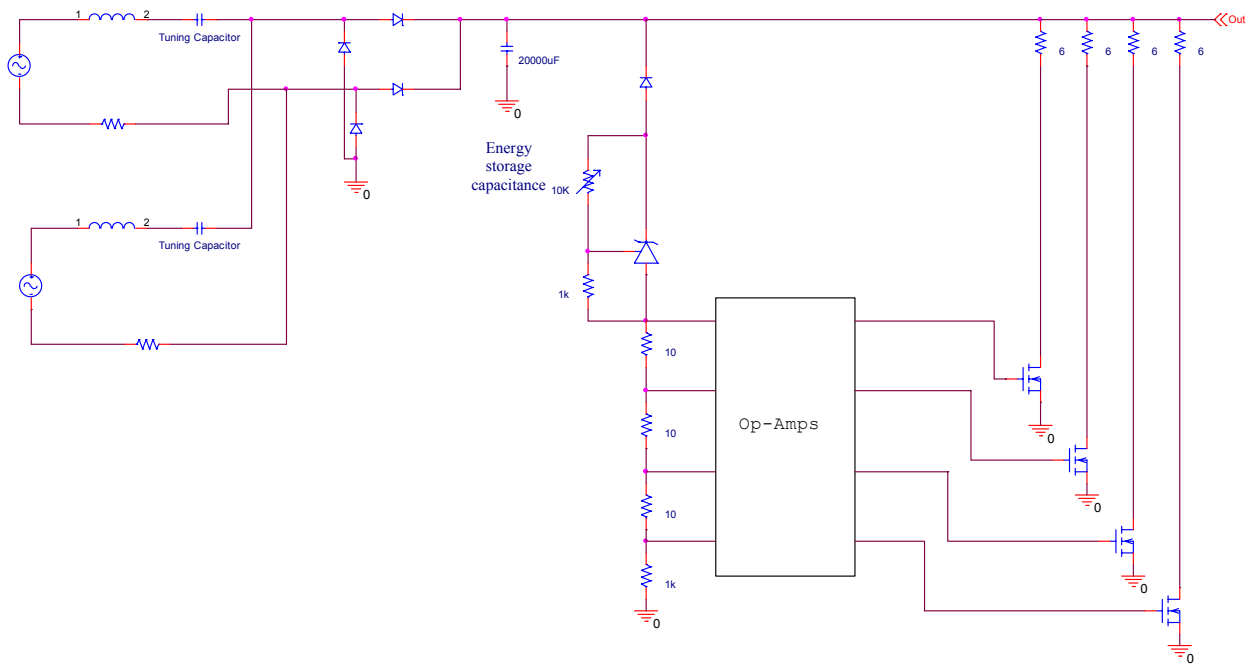


Figure 9.—Circuit model of zener-diode based controller

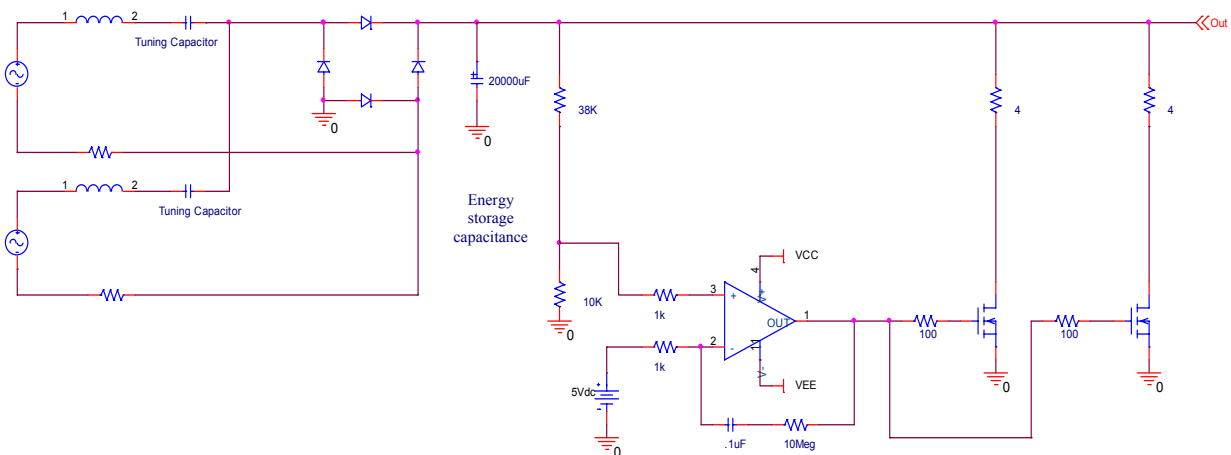


Figure 10.—Circuit model of linear DC voltage regulator controller

alternators is converted to DC. However, the DC voltage is sensed by a voltage divider connected to a single operational amplifier configured as a proportional-integral controller. It generates a voltage proportional to the difference between the divided voltage and the reference voltage. This output is used to drive FETs in their linear range, rather than discrete on-off states. The output of the operational amplifier controls the percentage activation of the FETs. The FETs connect load resistors onto the DC bus, but also dissipate power themselves. The user may change piston amplitude by adjusting the voltage divider that controls the input to the operational amplifier.

3. Digital Hybrid (Fig. 11)

The digital hybrid controller is similar to the zener-diode. The load can be adjusted in discrete steps, but not all steps are identical. Instead, the resistors are sized to provide a linear change in load. Also, the load is only updated once every half cycle of operation when the AC voltage crosses zero. The DC bus voltage is sensed by a voltage divider connected to an operational amplifier acting as a PID controller. The output of the PID loop is converted to a binary value by an analog-to-digital converter. The analog-to-digital converter is controlled by a zero crossing detector which generates a pulse each time the AC voltage crosses zero. The binary value controls FETs that switch resistors onto the DC bus. Any bit with a value of one will switch on the FET occupying the same position in the

sequence as the bit. The resistors are sized so that each provides twice the load as the previous one. As the DC voltage increases, the binary value increases, which applies more load to the DC bus. The user may change piston amplitude by adjusting the voltage divider that controls the input to the PID loop.

4. Buck Circuit With Zener-Diode (Fig. 12)

The AC from the alternators is rectified by a diode bridge. However, the energy storage capacitor for DC conversion is not connected directly to the diode bridge. Instead, an inductor, diode, and FET are inserted between the diode bridge and energy storage capacitor. These components, along with a pulse width modulator (PWM) comprise a buck circuit. The rectified AC voltage is sensed by a voltage divider connected to a PWM that switches the FET at 50 kHz. As the sensed voltage rises, the duty cycle of the PWM, and thus the FET, increases. When the FET is on, the AC is switched onto the buck circuit. The power flowing through the buck circuit must be dissipated and virtually any dissipative regulator will suffice. In this example, a zener-diode controller is used. The zener-diode controller functions the same as described above, but is used only to dissipate power. Coupling a buck circuit to a dissipative controller allows the load to be adjusted at a higher frequency than that of the alternator voltage. In this example, the load is adjusted 50,000 times each second. This allows the controller to respond more quickly to changes in convertor operation. One important consequence of this method is that the buck circuit reduces the output voltage below the desired range.

5. Boost Circuit With Pulse Width Modulation Regulator (Fig. 13)

This method operates similar to the buck circuit with zener-diode, but utilizes a boost circuit. The PWM still switches a FET at 50 kHz, but the FET connects a boost circuit. Again, power must be dissipated after the boost circuit. In this example, another PWM, FET, and resistor are used to provide load. The duty cycle of the FET is adjusted by the PWM to control the amount of load applied to the DC bus. This method also permits quicker adjustment of the load. One important consequence of this method is that the boost circuit increases the output voltage above the desired range.

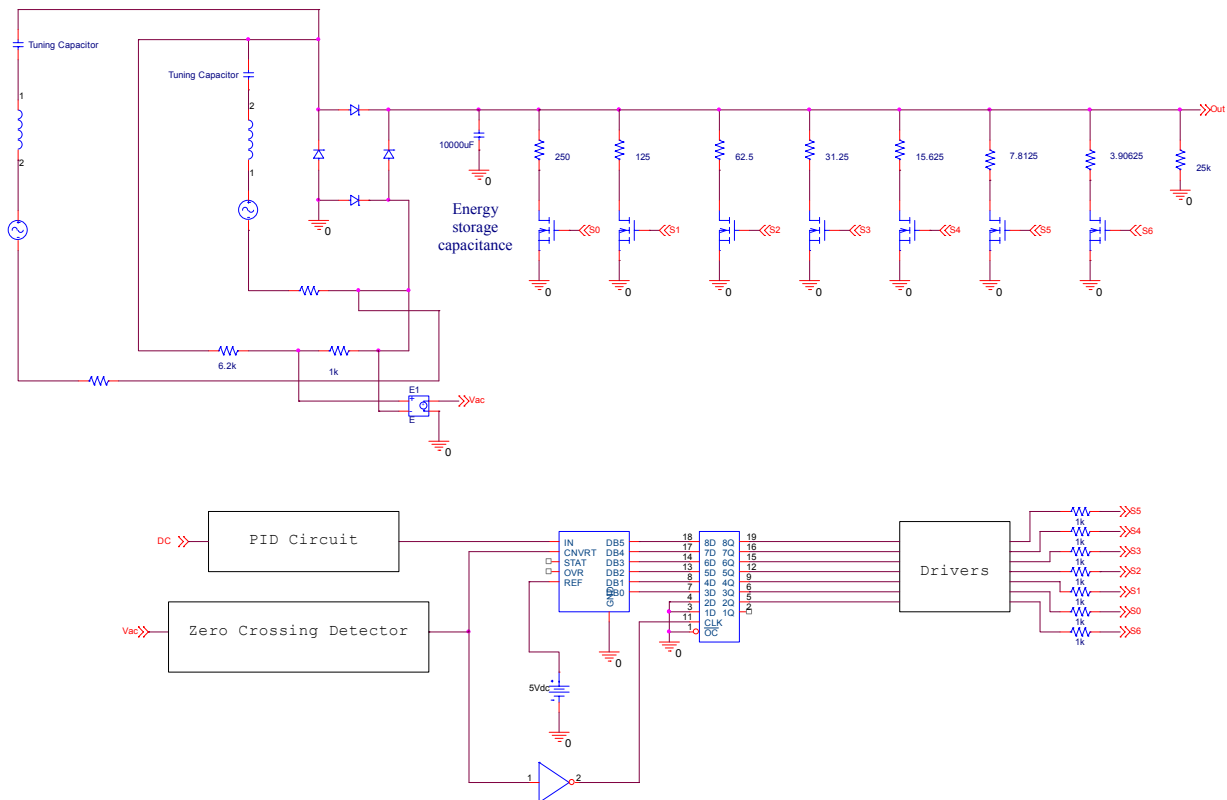


Figure 11.—Circuit model of digital hybrid controller

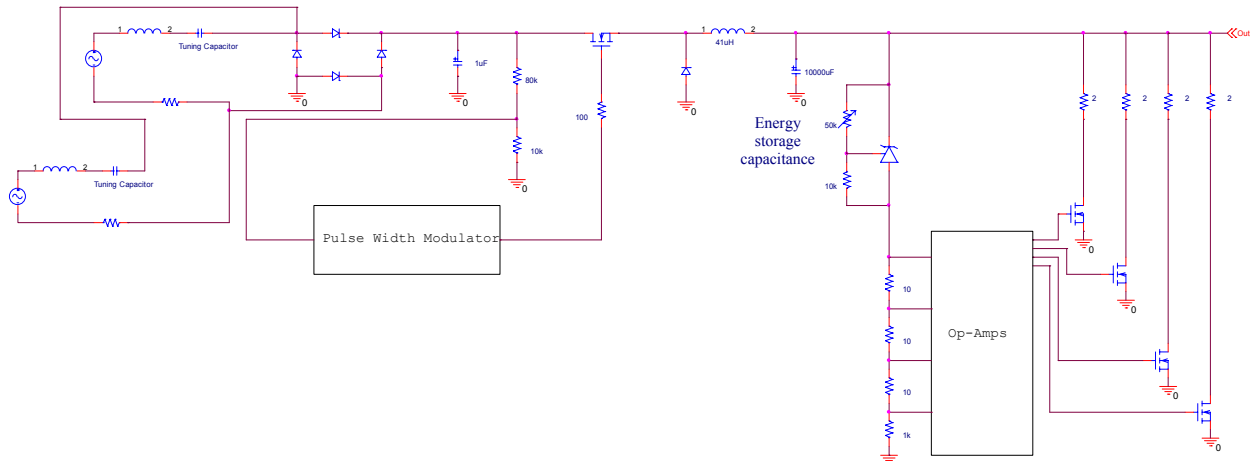


Figure 12.—Circuit model of buck circuit with zener-diode controller

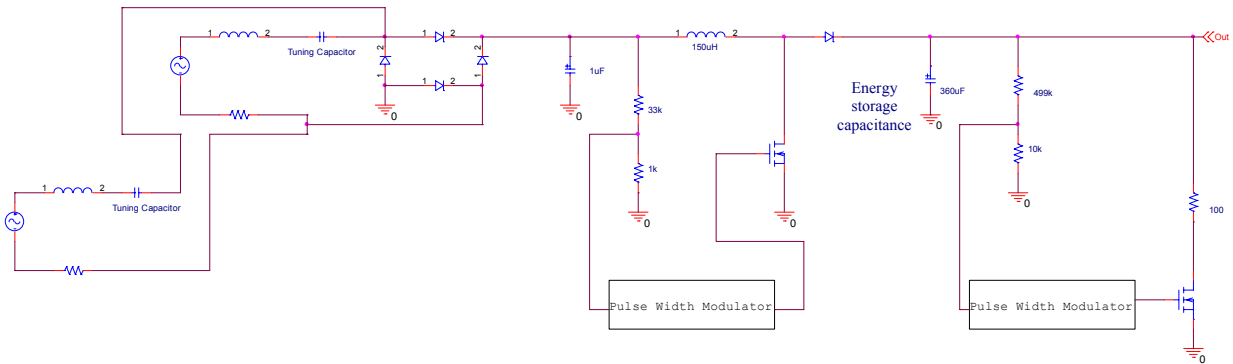


Figure 13.—Circuit model of boost circuit with pulse width modulator controller

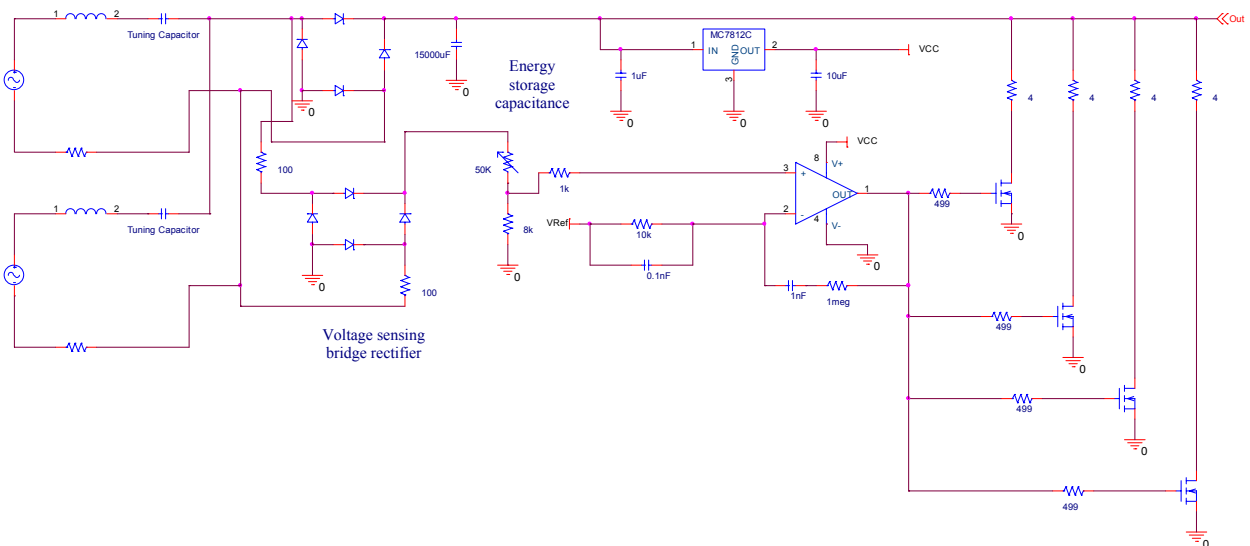


Figure 14.—Circuit model of linear AC regulator controller

6. Linear AC Regulator (Fig. 14)

This method operates in a manner similar to the linear DC voltage regulator method, except that the rectified alternator voltage is used to control the load instead of the DC voltage. The AC voltage is passed through a separate diode bridge with no energy storage capacitor that would convert it to DC. The remainder of operation is identical to the linear DC voltage regulator method. However, in this example, four FETs and load resistor sets are used instead of two.

C. Initial Evaluation

The initial controller option evaluation was based on results of PSpice modeling and general characteristics of each design. The circuit models were used to observe power dissipation in the loads, switching voltage, output voltage, and power flows. Observation of these items provided a first level indication of the performance of each option. Evaluation was also based on the criteria that follow.

The load can be controlled by monitoring either the AC or DC voltage. At a given frequency, the AC voltage is directly proportional to the piston amplitude. Therefore, the AC voltage is an accurate, real-time indicator of the piston motion. When the AC voltage is passed through the diode bridge rectifier, its full amplitude is still observable, but the waveform is altered so it occupies the positive region only. However, if the AC voltage is converted to DC by passing it through an energy storage capacitor, this amplitude is attenuated. The energy storage capacitor also has the effect of buffering changes in the alternator voltage output. Sudden changes in the AC voltage will be delayed because of the time constant of the capacitor. Therefore, AC bus voltage monitoring was considered desirable because it allows finer control of the load. The linear AC regulator, buck converter with zener-diode, and boost converter with PWM use AC bus monitoring. The zener-diode baseline, linear DC regulator, and digital hybrid use DC bus monitoring.

Staging refers to application of load by multiple circuits. Staging was considered desirable because it adds redundancy to the controller. Controllers can be designed to permit failure of at least one of the load connections while still maintaining stable operation full power. An example of load staging can be seen in the zener-diode based controller. As the DC bus voltage increases, each operational amplifier is activated in succession. If one of these loads loses connectivity, the duty cycle of the remaining circuits will be increased to compensate. The linear regulator options also use staging, but the load circuits are all activated the same percentage at a given time. If one of these loads loses connectivity, the percentage activation of the remaining circuits will be increased to compensate. The digital hybrid controller has multiple load circuits, but it cannot compensate for a loss of one of them. This is due to the fact that the loads are controlled by the binary number. If a connection to one load resistor were lost, the controller would attempt to compensate by increasing the binary number, but this would activate a larger load than necessary since each load is twice the magnitude of the previous one.

Power can be dissipated in either resistors or transistors. The reliability of a transistor is reduced when used to dissipate power. For example, the power dissipating capacity of a transistor is typically derated by 50 % for long-term, reliable operation. Because of this, use of resistors was considered desirable.

Some of the controller options required a DC-DC converter to return their output voltage to the desired range. The boost converter with PWM would normally output twice the linear alternator voltage. Similarly, the buck converter with zener-diode would normally output half the linear alternator voltage. A DC-DC converter is required on these two options to return the output voltage to 28 V_{DC}. The digital hybrid controller also requires a DC-DC converter to compensate for the relatively large overshoot in its output voltage due to the time constant of the PID loop. Use of a DC-DC converter was considered undesirable because it adds a relatively large component to the controller. Furthermore, the boost circuit with PWM was designed with power factor controller chip that operates directly off the rectified line voltage. No PSpice model was available for this chip, so this option could not be evaluated further.

Tuning refers to the process of customizing the controller for operation with a certain convertor design. This process is necessary to ensure stable output, proper power dissipation, and efficient switching of the FETs. Since each option was originally designed for TDCs, they required tuning for operation with ASCs and FTB convertors. Components that required customization during the tuning process include: load resistors and transistors, gate resistors, hysteresis resistor, voltage dividers, and energy storage capacitance. The buck and boost circuits made those controller options the most difficult to tune. The digital hybrid controller required extra tuning attention to the load resistors since they are not all the same like the other options. The zener-diode controller only required additional tuning of the hysteresis resistor on the operational amplifiers. The linear AC and linear DC regulator controllers did not require additional tuning.

Three of the six controllers were eliminated based on the advantages and disadvantages summarized in Table 3. The linear DC regulator method was eliminated because a design for linear AC regulation exists, and AC voltage monitoring was considered desirable. The boost circuit with PWM requires many more components than the other options, particularly a DC-DC converter. Also, the boost circuit with PWM couldn't be completely modeled in PSpice because of the use of the power factor controller. Therefore, the boost circuit option was not considered for evaluation any further. The baseline zener-diode and buck converter with zener-diode options both utilize load staging and dissipate power through resistors. However, the buck converter with zener-diode provides AC voltage control, making it more desirable, so the baseline zener-diode option was eliminated from further evaluation.

TABLE 3.—CONTROLLER OPTION QUALITATIVE EVALUATION SUMMARY.

Controller option	Advantages	Disadvantages	Eliminated
Zener-diode (baseline)	Resistor power dissipation Load staging	DC voltage monitoring	X
Linear DC regulator	Load staging	Transistor power dissipation DC voltage monitoring	X
Digital hybrid	Resistor power dissipation	Transistor power dissipation DC voltage monitoring DC-DC converter required	
Buck circuit with zener-diode	Resistor power dissipation AC voltage monitoring Load staging	DC-DC converter required Complex tuning	
Boost circuit with PWM	AC voltage monitoring	DC-DC converter required Complex tuning Lack of modeling capability	X
Linear AC regulator	AC voltage monitoring Load staging	Transistor power dissipation	

D. Further Evaluation

The three remaining controllers, linear AC regulator, buck circuit with zener-diode, and the digital hybrid were re-evaluated based on efficiency, parts count, sensitivity, and stability.

The power required to operate the controller is supplied by the convertors, which reduces the net usable power. Internal losses may be attributed primarily to housekeeping and inefficiencies of rectifier diodes. Housekeeping refers to the power required to operate the controller’s voltage dividers, operational amplifiers, and reference voltage supplies. Another significant source of power loss may occur in the diode bridge during rectification. For example, the baseline zener-diode controller discussed previously dissipates 26 W in the diodes when supplied 179 W (the maximum design power level). However, this can be reduced to 8 W by using Schottky diodes instead of silicone diodes. The full power efficiencies of the three remaining options, and the baseline zener-diode option, were calculated using the circuit models. The linear AC regulator, buck circuit with zener-diode, and digital hybrid efficiencies were calculated with a Schottky diode bridge. The zener-diode controller efficiency was calculated with a baseline silicon diode bridge. These values are summarized in Table 4.

Options with a larger number of components were considered less desirable. A higher part count decreases reliability, increases troubleshooting complexity, and may increase overall controller size. Identifying a failure is more difficult in a controller with a higher number of components. The buck circuit with zener-diode in particular required two potentiometers that must be set by the user, whereas the other options had only a single user adjustment. The overall controller volume can easily be dominated by the DC-DC converter and heat sinks. Options that do not require a DC-DC converter and fewer heat sinks were considered more desirable.

Since every electronic component has an associated tolerance, the sensitivity of each controller option to changes in component values was evaluated using the circuit models. It was found that the majority of sensitivity issues were caused by changes in the energy storage capacitor and load resistors. The energy storage capacitor had a rated tolerance of $\pm 20\%$, so in the circuit model the energy storage capacitance was varied between 8,000 and 12,000 μF . The results indicated that only the buck circuit with zener-diode was sensitive to changes in the energy storage capacitance. Modeling also revealed that only the digital hybrid controller was sensitive to changes in load resistance. This can be attributed to the fact that the load resistances of the digital hybrid controller must arranged in an ascending pattern. Each resistance is half the size of the previous one. In contrast, the load resistances of the other controller options may be identical.

Stability refers to the ability of the controller to maintain its output voltage at a fixed value when the convertor operating conditions change. A steady output voltage indicates the controller is able to maintain tight control of the piston amplitude. The circuit models were used to quantify the stability of each option by observing the ripple and overshoot of the output voltage.

Table 4 summarizes these criteria for each of the three remaining controllers and the baseline zener-diode controller. The values for voltage stability, and efficiency were calculated using the circuit models. The linear AC regulator was selected because of its favorable characteristics in almost every category. It exhibits the best voltage stability, requires the fewest components, and has the highest efficiency. The sole disadvantage of the linear AC regulator is its use of transistors for power dissipation. However, the risk associated with this was mitigated by designing the loads so the transistors would dissipate less than 50 % of their rated power capacity.

TABLE 4.—CONTROLLER OPTION QUANTITATIVE EVALUATION SUMMARY.

	Zener-diode (baseline)	Linear AC regulator	Digital hybrid	Buck converter with zener-diode
DC ripple (V)	0.3	0.08	0.5	0.4
DC overshoot (V)	1	1	11.2	0
Number of components	46	42	56	62
Heat sinks required	4	4	4	5
Sensitivity	None	None	Load resistance	Energy storage capacitance
Efficiency (%)	85.1	95.4	93.4	84.7

E. Linear AC regulator testing

Buildup of the linear AC regulator controller was completed in August 2006. Following this, a series of tests were conducted to check for functionality and characterize performance.

A checkout test was first conducted in August 2006. The controller was supplied power by an AC source to simulate single convertor input. A resistor was placed in series with the AC source to emulate the alternator resistance. This test confirmed the ability of the controller to dissipate 88 W. Measurements of output and operational amplifier voltages agreed well with model predictions, suggesting the PSpice models were valid.

A test was conducted to measure controller efficiency. Power was applied to the input of the controller using an AC voltage source to simulate convertor power. The voltage and current delivered to the input were measured to calculate power input. The voltage and current delivered to the loads were also measured to calculate power output. True-RMS meters were used for all measurements because the output voltage and current were non-sinusoidal. The output current meter was capable of measuring only up to 3 amps, which limited the maximum power input to 44 W_e for this test. At this power level, the efficiency was measured at 98.6%. This value agreed well with the model predictions, as summarized in Table 5. The circuit model predicted a controller efficiency of 95.5% at approximately 130 W_e, which is the maximum output of the ASRG simulator.

TABLE 5.—LINEAR AC REGULATOR EFFICIENCY SUMMARY

	Experimental	Theoretical (low power)	Theoretical (full power)
Power Input (W)	44.33	40.00	129.41
Power Output (W)	43.72	38.27	123.88
Efficiency (%)	98.64	95.68	95.49

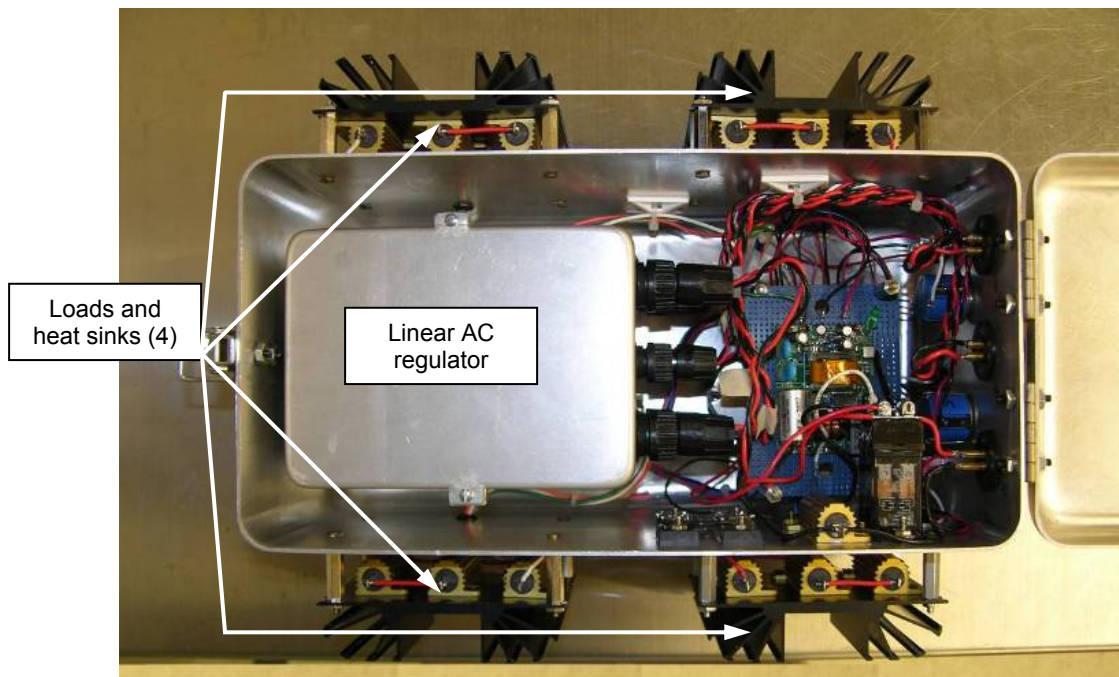


Figure 15.—Linear AC regulator controller integrated into ASRG simulator support electronics.

To verify functionality on operating convertors, the controller was tested on a pair of Sunpower, Inc. EE-35 units. Stable operation of the EE-35 units was demonstrated up to their maximum combined power output of 60 W_e. Voltage measurements agreed well with the model predictions.

Following successful checkout on the EE-35B convertors, the linear AC controller was integrated into the ASRG simulator electronics support, as discussed in section III. Stable operation of the FTB convertors was demonstrated up to their maximum combined power output of 130 W_e. However, the efficiency and stability at this condition remain to be measured. Stability was qualitatively evaluated by observing the linear alternator voltage. While operating at full power, the alternator voltage did not deviate more than 1 mV. A photograph of the controller integrated into the support electronics can be seen in Fig. 15. The controller occupies the left half of the container. The loads and their heat sinks are located on the outer surfaces of the container.

Plans have been made to replace the sensing diode bridge in the linear AC regulator with a true RMS-to-DC converter. This component computes the true root-mean-square value of a non-sinusoidal AC input signal and gives an equivalent DC output level. The true RMS value of a waveform is a more useful quantity than the average rectified value since it relates directly to the power of the signal. This modification theoretically eliminates the need for the user to constantly adjust the potentiometer.

V. Conclusion

A discussion of ASC testing at NASA GRC has been presented. The Stirling Research Lab has the capability to support simultaneous operation of up to eight ASC's in continuous, unattended mode. Three different testing configurations have been designed and implemented. ASC's may be operated continuously in an air or thermal vacuum environment. An ASRG simulator is also available for demonstration outside the research lab environment. A controller was designed and fabricated in-house after evaluation of six different options. This controller was functionally demonstrated on operating convertors, and then integrated into the ASRG simulator support equipment. ASC-0 nos.1 and 2 successfully operated in-air at full design conditions for 600 hr. The units were then transferred to thermal vacuum operation and have operated there for over 1000 hr as of June 2007. Beginning the summer of 2007, a pair of ASC-1HS units with a hot-end operating temperature of 850 °C will begin extended operation as well.

References

¹Chan, J., "Development of Advanced Stirling Radioisotope Generator for Space Exploration," proceedings of *Space Technology and Applications International Forum (STAIF-2007)*, edited by M.S. El-Genk, Albuquerque, NM, 2007.

²Schreiber, J.G., "Final Results for the GRC Supporting Technology Development for the 110-Watt Stirling Radioisotope Generator (SRG110)," proceedings of *Space Technology and Applications International Forum (STAIF-2007)*, edited by M.S. El-Genk, Albuquerque, NM, 2007.

³Schreiber, J.G., "Summary of Stirling Convertor Testing at GRC," *Proceedings of 4th International Energy Conversion Engineering Conference*, San Diego, CA, 2006, AIAA-2006-4061.

⁴Wood, J.G., "Advanced Stirling Convertor Phase II Achievements and Planned Phase III Effort," *Proceedings of 4th International Energy Conversion Engineering Conference*, San Diego, CA, 2006, AIAA-2006-4108.

⁵Schreiber, J.G., Roth, M., and Pepper, S.V., "Extended Operation of Stirling Convertors," *Proceedings of 2nd International Energy Conversion Engineering Conference*, Providence, RI, 2004, AIAA-2004-5508.

⁶Oriti, S.M., "Update on Extended Operation of Stirling Convertors in Thermal Vacuum at NASA Glenn Research Center," *Proceedings of 4th International Energy Conversion Engineering Conference*, San Diego, CA, 2006, AIAA-2006-4062, NASA/TM—2006-214424.

REPORT DOCUMENTATION PAGE

Form Approved
OMB No. 0704-0188

The public reporting burden for this collection of information is estimated to average 1 hour per response, including the time for reviewing instructions, searching existing data sources, gathering and maintaining the data needed, and completing and reviewing the collection of information. Send comments regarding this burden estimate or any other aspect of this collection of information, including suggestions for reducing this burden, to Department of Defense, Washington Headquarters Services, Directorate for Information Operations and Reports (0704-0188), 1215 Jefferson Davis Highway, Suite 1204, Arlington, VA 22202-4302. Respondents should be aware that notwithstanding any other provision of law, no person shall be subject to any penalty for failing to comply with a collection of information if it does not display a currently valid OMB control number.

PLEASE DO NOT RETURN YOUR FORM TO THE ABOVE ADDRESS.

1. REPORT DATE (DD-MM-YYYY) 01-11-2007		2. REPORT TYPE Technical Memorandum		3. DATES COVERED (From - To)	
4. TITLE AND SUBTITLE Advanced Stirling Convertor Testing at NASA Glenn Research Center				5a. CONTRACT NUMBER	
				5b. GRANT NUMBER	
				5c. PROGRAM ELEMENT NUMBER	
6. AUTHOR(S) Oriti, Salvatore, M.; Blaze, Gina, M.				5d. PROJECT NUMBER	
				5e. TASK NUMBER	
				5f. WORK UNIT NUMBER WBS 138494.04.01.01	
7. PERFORMING ORGANIZATION NAME(S) AND ADDRESS(ES) National Aeronautics and Space Administration John H. Glenn Research Center at Lewis Field Cleveland, Ohio 44135-3191				8. PERFORMING ORGANIZATION REPORT NUMBER E-16190	
9. SPONSORING/MONITORING AGENCY NAME(S) AND ADDRESS(ES) National Aeronautics and Space Administration Washington, DC 20546-0001				10. SPONSORING/MONITORS ACRONYM(S) NASA	
				11. SPONSORING/MONITORING REPORT NUMBER NASA/TM-2007-215010	
12. DISTRIBUTION/AVAILABILITY STATEMENT Unclassified-Unlimited Subject Category: 20 Available electronically at http://gltrs.grc.nasa.gov This publication is available from the NASA Center for AeroSpace Information, 301-621-0390					
13. SUPPLEMENTARY NOTES					
14. ABSTRACT The U.S. Department of Energy (DOE), Lockheed Martin Space Systems (LMSS), Sunpower Inc., and NASA Glenn Research Center (GRC) have been developing an Advanced Stirling Radioisotope Generator (ASRG) for use as a power system on space science and exploration missions. This generator will make use of the free-piston Stirling convertors to achieve higher conversion efficiency than currently available alternatives. The ASRG will utilize two Advanced Stirling Convertors (ASC) to convert thermal energy from a radioisotope heat source to electricity. NASA GRC has initiated several experiments to demonstrate the functionality of the ASC, including: in-air extended operation, thermal vacuum extended operation, and ASRG simulation for mobile applications. The in-air and thermal vacuum test articles are intended to provide convertor performance data over an extended operating time. These test articles mimic some features of the ASRG without the requirement of low system mass. Operation in thermal vacuum adds the element of simulating deep space. This test article is being used to gather convertor performance and thermal data in a relevant environment. The ASRG simulator was designed to incorporate a minimum amount of support equipment, allowing integration onto devices powered directly by the convertors, such as a rover. This paper discusses the design, fabrication, and implementation of these experiments.					
15. SUBJECT TERMS Stirling; Radioisotope					
16. SECURITY CLASSIFICATION OF:			17. LIMITATION OF ABSTRACT	18. NUMBER OF PAGES	19a. NAME OF RESPONSIBLE PERSON
a. REPORT	b. ABSTRACT	c. THIS PAGE			STI Help Desk (email:help@sti.nasa.gov)
U	U	U	UU	23	19b. TELEPHONE NUMBER (include area code) 301-621-0390

